Available online at www.sciencedirect.com
ScienceDirect
Journal of the European Ceramic Society 29 (2009) 2903–2913
www.elsevier.com/locate/jeurceramsoc

Characterisation of glasses in the TeO_2–WO_3–PbO system

D. Munoz-Martín [a], M.A. Villegas [b,*], J. Gonzalo [a], J.M. Fernández-Navarro [a]

[a] *Laser Processing Group, Instituto de Óptica, Consejo Superior de Investigaciones Científicas (CSIC), C. Serrano, 121, 28006 Madrid, Spain*
[b] *Instituto de Historia, CCHS, Consejo Superior de Investigaciones Científicas (CSIC), C. Albasanz, 26-28, 28037 Madrid, Spain*

Received 5 December 2008; received in revised form 6 April 2009; accepted 16 April 2009
Available online 17 May 2009

Abstract

As potential candidates for photonic devices, non-linear materials and coatings, 22 glasses in the TeO_2–WO_3–PbO system have been formulated and prepared by conventional melting at temperatures ranging between 710 and 750 °C. The glass forming area has been determined for a wide region of the corresponding ternary diagram. Structural characterisation of the glasses was conducted through FTIR spectrometry and the variation of density values, which allowed calculation of the glass molar volume and the oxygen molar volume. UV–VIS spectra were recorded to determine optical absorption/transmission and energy gap values. Likewise, such results were correlated with the glasses composition and their ability for optical materials. DTA curves yielded data of transition temperature (T_g), onset crystallisation temperature (T_c) and the thermal stability range of glasses. Crystalline phases formed in devitrified and partially devitrified glasses were detected by X-ray diffraction. The properties and structural features of glasses were discussed in terms of their relative proportion of former/modifier oxides. The main glass former oxide is TeO_2, which arranges [TeO_4] groups with tetrahedral coordination, while PbO plays as glass modifier oxide. Tungsten oxide is incorporated as network former, alternating with TeO_2 and forming mixed linkages Te–O–W and W–O–W. WO_3 is the component that contributes most to increase the glass transition temperature, and to decrease both the oxygen molar volume and the thermal expansion coefficient.

Keywords: Tellurite glasses; Structure; Thermal properties; Optical spectroscopy

1. Introduction

Among the glass families investigated for photonic applications, tellurite glasses are of great interest because of their promising optical properties (high refractive index, low phonon energy, wide transmission in the infrared range and high non-linear behaviour, able for developing ultrafast switching in optical devices), due to the high polarisability of the Te^{4+}-ions, which possess a non-bonding electron lone pair $5s^2$. For enhancing the optical behaviour of tellurite glasses, other heavy metals oxides or oxides with empty *d* orbitals, such PbO, Bi_2O_3, TiO_2 and Nb_2O_5 have been incorporated.

Following the research line of a former work,[1] the purpose of this research is the study of properties of glasses in the TeO_2–WO_3–PbO ternary system, on the basis of their possible application as base materials for photonic devices. This system allows, on the one hand, obtaining glasses with wide composition range, since these three oxides are suitable to become glass network formers. On the other hand, due to their high polarisability, each one of these three components could contribute in a great extent to the obtaining of high refractive index glasses and enhanced non-linear optical properties.

Binary tellurite–tungstate glasses have been studied by Vogel et al.,[2] Yakhkind,[3] Al-Ani et al.,[4] Dimitrov,[5] El-Mallawani,[6] Charton et al.,[7] Shaltout et al.[8,9] and Sokolov et al.[10] Ternary tellurite–tungstate glass systems with alkaline oxides,[11–13] zinc oxide,[14,15] bismuth oxide[16,17] or lanthanum oxide[13,18] as third components, or other complex multicomponent glasses[19–21] have demonstrated to be excellent hosts for Er^{3+} and Yb^{3+}-ions and very promising materials for developing broadband integrated optical amplifiers.

First glasses in the TeO_2–WO_3–PbO system were obtained by Stanworth[22] in a wide preliminary study about tellurite glasses of different compositions, including their properties. Then Heckroodt and Res[23] studied some properties of these glasses as matrices for incorporating high contents of Er_2O_3. More recently the elastic moduli and the ultrasonic characterization of glasses of this ternary system have been studied by Afifi et al.[24,25]

* Corresponding author. Tel.: +34 916022672; fax: +34 916022971.
E-mail address: mariangeles.villegas@cchs.csic.es (M.A. Villegas).

0955-2219/$ – see front matter © 2009 Elsevier Ltd. All rights reserved.
doi:10.1016/j.jeurceramsoc.2009.04.018

2. Experimental

2.1. Glasses composition and preparation

Ten grams batches of every sample (nominal compositions are summarised in Table 1) were prepared by mixing the corresponding high purity oxides (TeO_2 Alfa 99.99; WO_3 Aldrich 99.995 and PbO Aldrich 99.999) in an agate balls mill. The powder mixture was put in a platinum crucible and heated in an electrical vertical furnace Thermostar® at temperatures in the 710–750 °C range. Glass melts were homogenised by using an electrical platinum stirrer and after 45 min the glasses were poured onto a preheated brass mould. The obtained glass blocks (about 1 cm^3 size) were immediately introduced into the annealing furnace, kept for 15 min at temperatures ranging from 350 to 400 °C and then cooled down to room temperature at 3 °C min^{-1}. Sample nos. 3, 17, 18, 20 and 22 resulted partially crystallised. All the other samples yielded from yellow to orange homogeneous transparent glasses free of strains. The absence of crystalline phases in all these transparent samples was confirmed by X-ray diffraction. Only wide diffuse bands centred at about $2\theta = 20–35^\circ$ can be observed in all X-ray diffraction patterns.

2.2. Characterisation techniques

Crystalline phases of the devitrified glass samples prepared were identified by X-ray diffraction (XRD). A Siemens D 5000 equipment was used (Kα of Cu, 40 kV, 30 mA, $2\theta = 2–60^\circ$).

The densities of glasses (Table 1) were determined at 23 °C by the immersion method using trichloroethylene as immersion liquid. The experimental data obtained are affected by a maximum error of 0.4%. Thus, all the other values calculated from densities (V_M, V_O) would have the same error.

Table 1
Composition (mol%) and densities of the prepared glasses.

Sample number	TeO_2	WO_3	PbO	ρ (g cm^{-3}) at 23 °C
1	90	10	0	5.798
2	90	5	5	5.867
3	90	0	10	crystallised
4	85	15	0	5.890
5	85	0	15	6.090
6	80	20	0	5.951
7	80	15	5	6.056
8	80	10	10	6.128
9	80	5	15	6.184
10	80	0	20	6.282
11	75	15	10	6.221
12	75	5	20	6.410
13	70	20	10	6.313
14	70	10	20	6.488
15	60	30	10	6.519
16	60	20	20	6.663
17	60	10	30	crystallised
18	50	40	10	crystallised
19	50	30	20	6.831
20	50	20	30	partially crystallised
21	40	40	20	7.018
22	40	30	30	crystallised

Transition temperature T_g and thermal stability data were obtained from differential thermal analyses (DTA), which were carried out under N_2 atmosphere at a heating rate of 10 °C min^{-1}, using a TA Instruments/SDT 600 system, with a maximum error of 3 °C.

The linear expansion coefficients $\alpha_{100–250^\circ C}$ were determined from dilatometric curves recorded with a dilatometer model TMA-Q400 of TA Instruments, at a heating rate of 10 °C min^{-1}. The experimental values are affected by a maximum error of 0.5%.

From the glass blocks obtained, planoparallel slabs about 1 mm thick were cut and optically polished. Their optical absorption/transmission spectra were recorded in the 300–1000 nm wavelength range, using an Ocean Optics spectrophotometer model HR4000CG-UV-NIR. Transmittance values to be further used for the energy gap (E_g) calculations were corrected for the standard thickness of 1 mm.

Infrared spectra were recorded with a 20SXC FT-IR spectrometer with a resolution of 2 cm^{-1} in the 300–1300 cm^{-1} range. KBr pellets technique was used for recording spectra of glasses.

3. Results and discussion

3.1. Glass forming area

For each composition system the limits of the glass forming area depend on the preparation conditions, particularly on the cooling down rate. This explains why in the binary system TeO_2–WO_3, Vogel et al.[2] could prepare glasses containing WO_3 in the 11.5–30.8 mol% range; El-Mallawany[5] between 11.0 and 33.3 mol% WO_3; Charton et al.[7] could introduce up to 32.5 mol% WO_3, Al-Ani et al.[4] up to 33 mol% WO_3 and Shaltout et al.[8] up to 50 mol% WO_3.

In the binary system TeO_2–PbO the glass forming range is smaller. Vogel et al.[2] determined the range 13.6–20.8 mol% PbO, while El-Mallawany[6] determined the range 5.0–20.0 mol% PbO and Silva et al.[26] up to 50 mol% PbO.

Fig. 1 shows the composition of the samples prepared in the ternary system TeO_2–WO_3–PbO. The glass forming area agrees with that investigated by Heckroodt and Res[20] for such system. Black points correspond to devitrified glasses in which several crystalline phases were identified by XRD (Table 2).

3.2. FTIR spectra

Both in crystalline TeO_2 and tellurite glasses, Te^{4+}-ions form [TeO_4] groups in trigonal bipiramyds (tbp).[5] In such structures two oxygen ions are located in the axial vertices, while the other two oxygen ions and the lone electron pair of tellurium are located in the three equatorial positions. The equatorial Te–O bonds are slightly shorter than the axial bonds, as indicated Kim and Yoko.[27] Trigonal bipiramyds are linked one each other by sharing their vertices and forming a continuous three-dimensional structure.

The spectrum of crystalline TeO_2 is dominated by two main bands (Table 3): one of them is a wide asymmetric band at

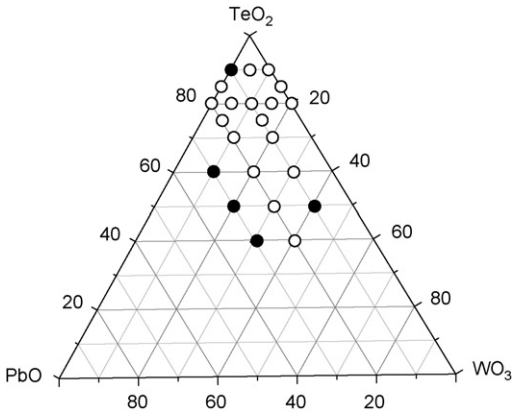

Fig. 1. Ternary diagram for the TeO_2–WO_3–PbO system showing the composition of the samples prepared. Hollow (◯) points correspond to homogeneous glasses and full (●) points to devitrified samples.

Table 2
Crystalline phases detected by XRD in devitrified samples.

Sample number	Crystalline phases detected	Formulae
3	Tellurium oxide	α-TeO_2
	Tellurium tungsten oxide	$Te_{0.95}W_{0.05}O_{2.05}$
	Lead tellurium oxide	$Pb_2Te_3O_7$
	Litharge	PbO
	Tungsten oxide	WO_3
17	Lead tellurate	$PbTe_3O_7$
18	Tungsten oxide	WO_3
20	Stolzite	$PbWO_4$
	Lead tellurate	$PbTe_3O_7$
22	Stolzite	$PbWO_4$

650–660 cm^{-1} and the other is a narrow symmetric band at 775 cm^{-1}. Following Armand and Charton,[28] the first band is due to axial symmetric vibrations of $Te–O_{ax}$ bonds, while the band at 775 cm^{-1} is due to equatorial asymmetric vibrations of $Te–O_{eq}$ bonds.

In the spectra of tellurite glasses, the band at 650 cm^{-1} appears very much broader, due to their disordered structure, which causes the 775 cm^{-1} band to appear as a shoulder.

3.2.1. Binary glasses

The incorporation of network modifier ions into a tellurite glass enhances the breaking of axial Te–O–Te linkages in the trigonal [TeO_4] bipiramyds (tbp). This causes the appearing of [TeO_3] (tp) units and the formation of non-bridging oxygens.

Table 3
Assignments of FTIR bands.

Wavenumber (cm^{-1})	Assignment
650–660	$Te–O_{ax}$ in [TeO_4]
775	$Te–O_{eq}$ in [TeO_4]
633, 695 (shoulders)	$Te–O^-$
700–800	W–O–W
800–860	W–O–W
905–930	W–O in [WO_4] or [WO_6]

Table 4
Coordination index, ionic radius and field intensity of the components of the studied glasses.

Ion	Coordination index	Ionic radius (nm)	Field intensity
Te^{4+}	6	0.097	0.71
Pb^{2+}	6	0.132	0.27
Pb^{2+}	8	0.137	0.26
W^{6+}	6	0.062	1.47
W^{6+}	4	0.059	1.52
O^{2-}	–	0.140	–

The spectrum (not shown) of the partially crystallised sample 3 ($90TeO_2{\cdot}10PbO$) (see Table 2) clearly shows the bands of crystalline TeO_2 at 657 and 773 cm^{-1}, plus two weak shoulders at about 633 and 695 cm^{-1}. When the PbO molar percentage increases substituting TeO_2 in the samples $85TeO_2{\cdot}15PbO$ and $80TeO_2{\cdot}20PbO$, both bands shift towards lower frequency and they appear broader, in such a way they overlap with the two weak shoulders mentioned above. This shift could be attributed to the Pb^{2+}-ions incorporation as network modifiers, which form new non-bridging oxygens in $Te–O^-\ldots Pb^{2+}\ldots{}^-O–Te$ linkages. The higher polarisability of such new non-bridging oxygens explains the bands shift towards lower frequency, due to the lower field intensity of Pb^{2+}-ions (0.27) compared with that of Te^{4+}-ions (0.71) (Table 4).

Tungsten ions have an intermediate behaviour between network formers and modifiers. Thus, depending on the own nature of the other glass components in the three-dimensional structure and on their percentage, they could play the role of formers or modifiers. In binary TeO_2–WO_3 glasses, tungsten ions should play as network modifiers, while in ternary glasses TeO_2–WO_3–PbO they could most likely play the role of network formers.

The incorporation of WO_3 into tellurite glasses causes both the diminishing of trigonal bipiramyds (tbp) and the forming of non-bridging oxygens.[6,29–31] In binary TeO_2–WO_3 glasses the band at 650 cm^{-1} due to $Te–O_{ax}$ vibrations also shifts slightly towards lower frequencies. This can be attributed to the formation of non-bridging oxygens $Te–O^-$ that, in addition, cause the progressive band broadening.

Moreover, the incorporation of WO_3 induces the appearing of two shoulders at 700–800 and 800–860 cm^{-1}, and a well defined band in the 905–930 cm^{-1} range. All the former vibrations are included in the reference spectrum of γ-WO_3. The structural network of this compound is formed by octahedral [WO_6] units, which share their vertices. The shoulder at 860 cm^{-1} is assigned to the vibration of W–O–W linkages,[29] while the band at 905–930 cm^{-1} is due to tetrahedral [WO_4] units or octahedral [WO_6] units, since it appears in crystalline tungstates with small frequency variation for tungsten ions adopting tetrahedral or octahedral coordination.[9] This band shifts towards higher frequency when the WO_3 percentage increases and it was attributed[4] to a change of tungsten coordination, from [WO_4] to [WO_6] units. However, Charton et al.[7] concluded (by using XPS and XANES spectroscopies in binary TeO_2–WO_3 glasses containing up to 32.5 mol%) that W^{6+}-ions are always incor-

porated in tellurite glasses as octahedral [WO_6] units, and the observed shift towards higher frequency when WO_3 concentration increases are only due to a great distortion of such octahedral groups. El-Mallawany[6] assumed that the WO_3 incorporation does not affect the coordination of [TeO_4] groups.

Sokolov et al.[10] have studied the structure of WO_3–TeO_2 glasses by quantum-chemical simulation and Raman spectroscopy, concluding that both oxides build a continuous network formed by three types of structural groups: trigonal bypiramids, O=TeO_2 pyramids, and O=WO_5 octahedra, creating Te–O–Te, Te–O–W and W–O–W bonds. These authors considered tetrahedral coordinations [WO_4] not necessary to form the glass network.

3.2.2. Ternary glasses

In ternary glasses the bands shifts observed are even more important than in binary glasses when the WO_3 concentration varies. In this case, the simultaneous variation of a third component induces for a more deformable network.

All FTIR spectra of ternary glasses show the same features described for binary glasses. The characteristic main band at 650 cm^{-1} always appears, although its exact position depends on the composition. This indicates that the structure based on trigonal bipiramyds [TeO_4] (tbp) is maintained in all the glasses studied. Nevertheless, the incorporation of both WO_3 and PbO diminish the [TeO_4] (tbp)/[TeO_3] (tp) ratio, as a consequence of the increasing of non-bridging oxygens.

3.2.2.1. Ternary glasses with constant PbO content. For constant [PbO], the decreasing of the [TeO_2]/[WO_3] ratio in the series $(90-x)TeO_2{\cdot}xWO_3{\cdot}10PbO$ and $(80-x)TeO_2{\cdot}xWO_3{\cdot}20PbO$, i.e. the substitution mol by mol of TeO_2 by WO_3, causes an increase of networking oxygens, according to the proportion 3/2. Once incorporated into the glass network these oxygens form new Te–O–W and W–O–W linkages. Thus, the WO_3 incorporation yields a network distortion that can be monitored by the progressive broadening of the band at 650 cm^{-1} (Fig. 2a). Simultaneously, a strong shift of the band from 638 to 665 cm^{-1}

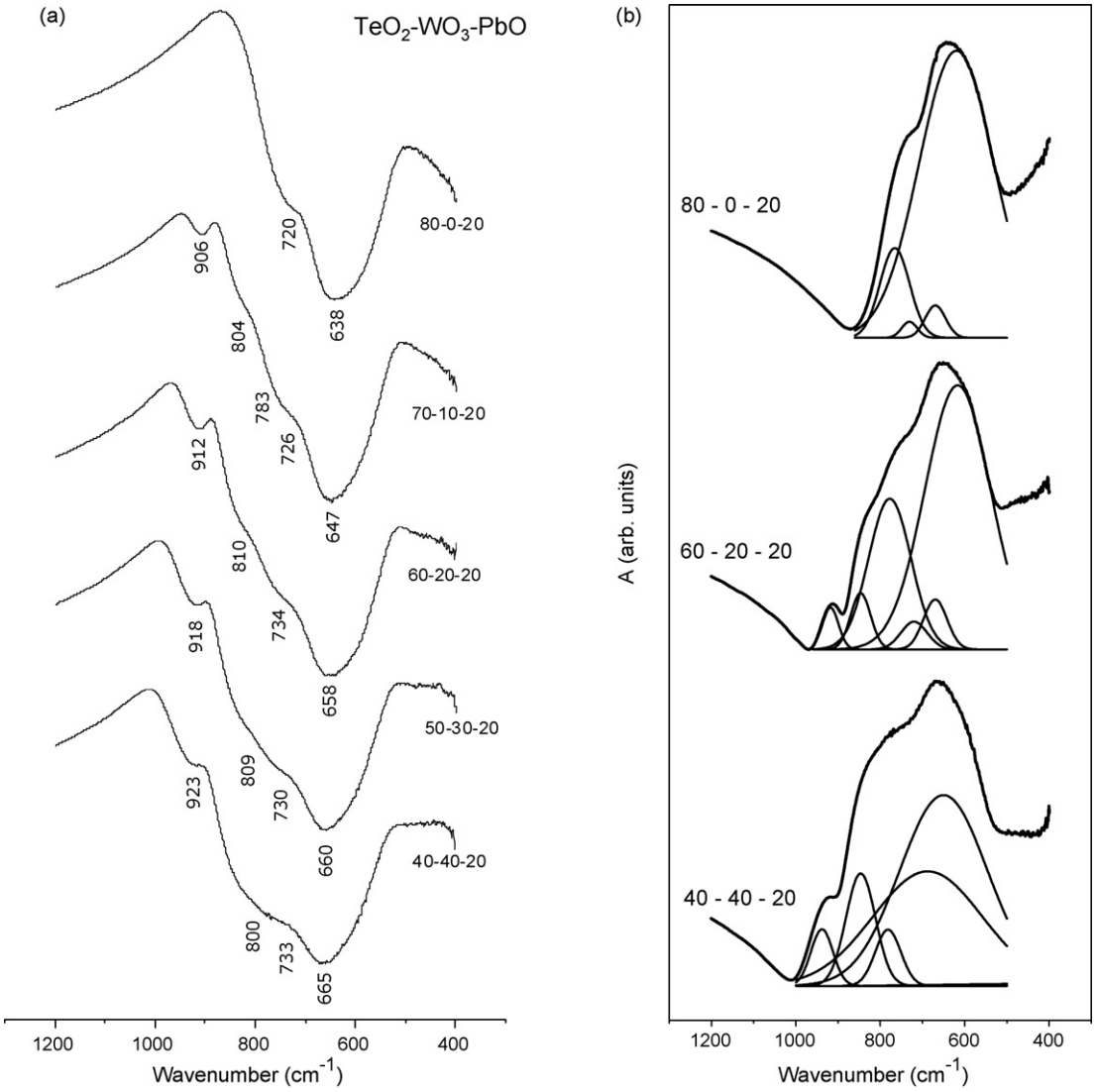

Fig. 2. (a) FTIR and (b) representative deconvoluted FTIR spectra of the ternary glass series $(80-x)TeO_2{\cdot}xWO_3{\cdot}20PbO$. Note that in order to show clearer the different bands, the deconvoluted spectra in (b) has sign reversed.

occurs. This is due to the higher field intensity of the mixed Te–O–W linkages, in which the oxygen is highly polarised, compared with Te–O–Te linkages, since W^{6+}-ions possess higher field intensity than Te^{4+}-ions. The band at 730 cm^{-1} corresponding to Te–O_{eq} bonds does not vary its position.

In the former two glass series the progressive incorporation of WO_3 gives rise to the appearing of the shoulder at 800–830 cm^{-1} and the band at 905–930 cm^{-1}, both attributed to W–O bonds. The shoulder does not vary in a great extent when WO_3 percentage increases; while the band clearly shifts towards 930 cm^{-1}. This shift has been also observed by Dimitrov[5] and Charton et al.,[7] even though their interpretations are quite different, as is said above.

Former qualitative discussion has been confirmed by deconvolution of all the corresponding spectra. In Fig. 2b the most representative deconvoluted spectra are shown.

3.2.2.2. Ternary glasses with constant TeO_2 content. In the glass series $90TeO_2{\cdot}xWO_3{\cdot}(10-x)PbO$, $80TeO_2{\cdot}xWO_3{\cdot}(20-x)PbO$ (Fig. 3a), $70TeO_2{\cdot}xWO_3{\cdot}(30-x)PbO$ and $60TeO_2{\cdot}xWO_3{\cdot}(40-x)PbO$ the band at 650 cm^{-1} assigned to $[TeO_4]$(tbp) and $[TeO_3]$(tp) groups also shifts towards higher frequency, when PbO is substituted by WO_3. However, this shift is smaller than the produced by the substitution of TeO_2 by WO_3. Therefore, in this case the network distortion is much lower. On the other hand, both the shoulder at 800 cm^{-1} and the band at 920 cm^{-1}, assigned to W–O bonds, shift towards higher wavenumbers. This is a consequence of the formation of new octahedral $[WO_6]$ units, due to the higher number of oxygens incorporated by the WO_3 and by the higher field intensity of Te–O–W and W–O–W linkages.

Fig. 3b shows some of the deconvoluted spectra of samples with constant TeO_2 (80 mol%), which support this interpretation.

3.2.2.3. Ternary glasses with constant WO_3 content. In the glass series $(80-x)TeO_2{\cdot}20WO_3{\cdot}xPbO$ (Fig. 4a and b) both the band at 650 cm^{-1} and the shoulder at 750 cm^{-1} slightly shift

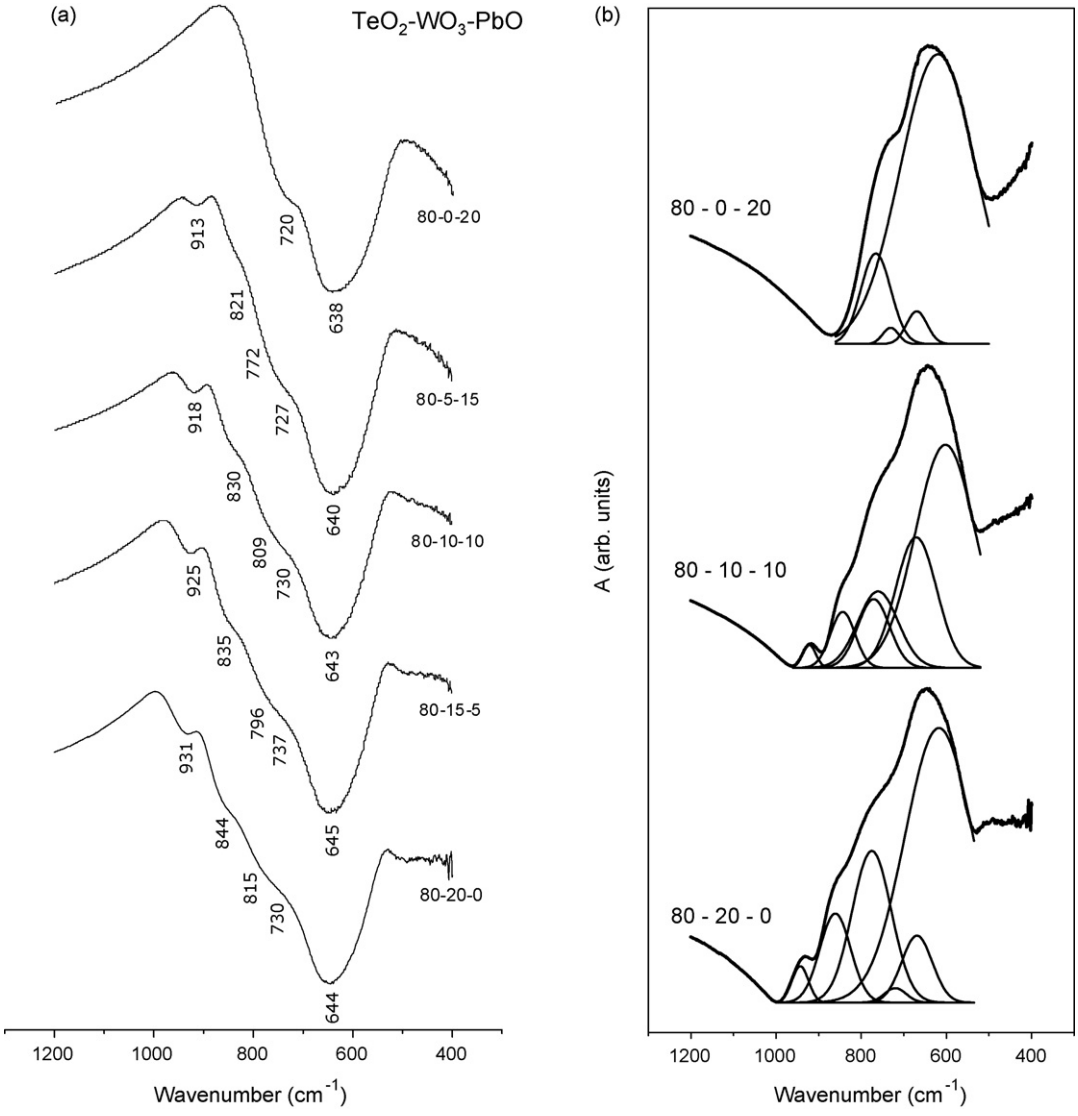

Fig. 3. (a) FTIR and (b) representative deconvoluted FTIR spectra of the ternary glass series $80TeO_2{\cdot}xWO_3{\cdot}(20-x)PbO$. Note that in order to show clearer the different bands, the deconvoluted spectra in (b) has sign reversed.

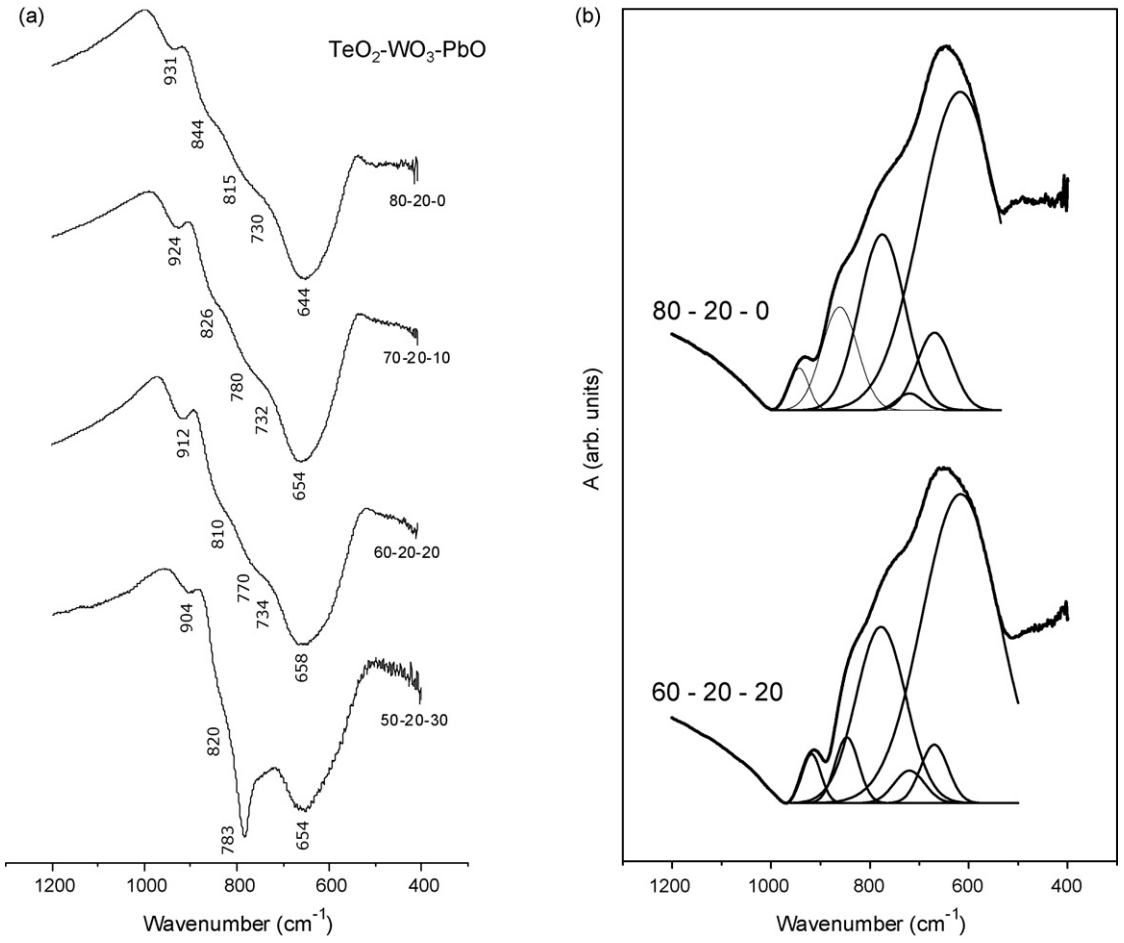

Fig. 4. (a) FTIR and (b) representative deconvoluted FTIR spectra of the ternary glass series $(80-x)TeO_2{\cdot}20WO_3{\cdot}xPbO$, (the sample 50–20–30 is partially crystallised). Note that in order to show clearer the different bands, the deconvoluted spectra in (b) has sign reversed.

when PbO percentage increases. In this case the deformation of the basic structure of the glass network is smaller, compared with the distortion caused by the substitution of TeO_2 by WO_3. When TeO_2 is substituted mol by mol by PbO, the number of oxygens in the glass network diminishes according to the ratio 2/1. Thus, the glass network becomes less distorted, less stressed and more closed. That is why for constant 20 mol% WO_3, the shoulder at 800 cm^{-1} and the band at 905–930 cm^{-1} shift towards lower wavenumber. In other words, more tetrahedral [WO_4] groups have been formed, which yield lower network distortion. This explanation agrees with the interpretation of Dimitrov.[5]

3.3. Molar volume and oxygen molar volume

3.3.1. Molar volume

The molar volume is calculated as a function of the molar fraction of each one of the three components. In Fig. 5 the variation of the molar volume as a function of X_{TeO_2} has been plotted for different molar percentages of PbO and WO_3. The molar volume of glasses decreases linearly when WO_3 is substituted mol by mol by TeO_2 (X_{PbO} = constant), but the slope progressively decays in the series with 0, 10 and 20 mol% PbO. This is explained because the substitution of WO_3 by TeO_2 diminishes the number of oxygen atoms in the ratio 2/3, being more important for the lowest TeO_2 contents. Thus, the highest value ($V_M = 29.25\ cm^3$) corresponds to the glass $80TeO_2{\cdot}20WO_3$, which is the glass with the highest percentage of oxygen atoms (this is the component with highest molar volume). The lowest value (27.43 cm^3) corresponds to the glass $80TeO_2{\cdot}20PbO$. Considering the variation of V_M as a function of X_{WO_3}, the molar

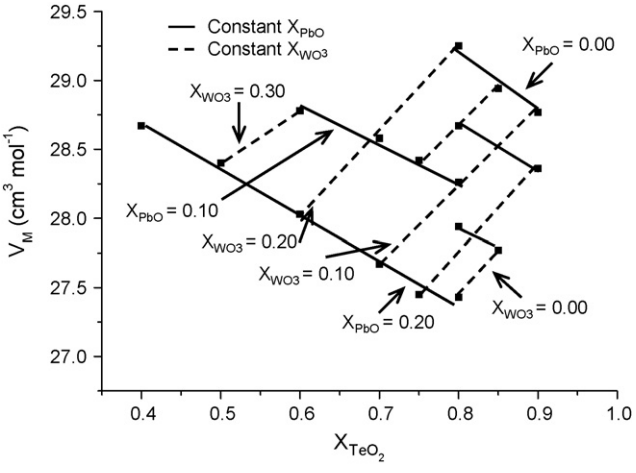

Fig. 5. Variation of the molar volume of glasses as a function of the TeO_2 molar fraction.

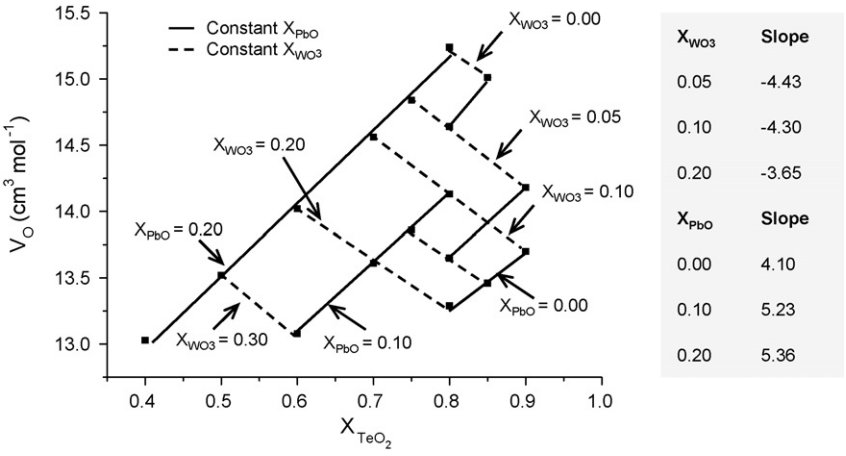

X_{WO3}	Slope
0.05	-4.43
0.10	-4.30
0.20	-3.65
X_{PbO}	Slope
0.00	4.10
0.10	5.23
0.20	5.36

Fig. 6. Variation of the oxygen molar volume of glasses as a function of the TeO_2 molar fraction. Continuous fitting lines correspond to constant X_{PbO} and dashed lines to constant X_{WO_3}. Representative values of the obtained slopes are included.

volume increases with [WO_3]. This component brings the higher number of oxygens, i.e. of ions with the higher volume, despite the W^{6+}-ions have the smallest radius.

3.3.2. Oxygen molar volume

Oxygen molar volume has been calculated following the expression:

$$V_O = \left(\sum \frac{x_i M_i}{\rho}\right)\left(\frac{1}{\Sigma x_i n_i}\right) \quad (1)$$

where x_i is the molar fraction of each component i; M_i is the molecular weight; ρ the glass density and n_i the number of oxygen atoms in each oxide.

For constant PbO concentration, when TeO_2 is substituted mol by mol by WO_3, the oxygen molar volume V_O decreases linearly (Fig. 6). In other words, the glass structure becomes more densified. The oxygen ions in the new mixed Te–O–W and W–O–W linkages are more polarised than the oxygen ions in Te–O–Te linkages, due to the higher field intensity of W^{6+}-ions (1.47), respect to the field intensity of Te^{4+}-ions (0.71) (Table 4). This yields a more compact packing of the oxygen ions. For a constant PbO content (20 mol%), the resulting decrease of V_O varies almost linearly between 4.5% and 3.6% per each 10 mol TeO_2 that are substituted by 10 mol WO_3. For a given constant WO_3 molar percentage (20 mol%), V_O diminishes with the molar percentage of TeO_2, respect to the content of PbO. This can be also explained by the higher field intensity of Te^{4+}-ions (0.71), compared with the field intensity of Pb^{2+}-ions (0.26–0.27; Table 4). For constant molar percentages of WO_3, the decrease of V_O varies between 3.8 and 3.9% per each 10 mol PbO substituted by 10 mol TeO_2. In Fig. 6 the slopes of the linear fits for different values of X_{PbO} and X_{WO_3} are indicated. The slope values increase with X_{PbO} while they decrease when increasing X_{WO_3}. In this case the difference of their corresponding field intensities is higher than in former cases.

The largest V_O decrease is observed when PbO is substituted by WO_3 for constant molar percentages of TeO_2. In this case the difference of their corresponding field intensities is higher than in former cases.

3.4. Thermal properties

3.4.1. Glass transition temperature

The transition temperature (T_g) gives information on both the strength of interatomic bonds and the glass network connectivity, in a similar way that the melting temperature does it for crystalline solids. T_g of the glasses studied in the present work varies linearly with the molar fraction of each one of the three components (Fig. 7). The maximum variation occurs when TeO_2 is substituted mol by mol by WO_3 in the glass series $(80-x)TeO_2{\cdot}xWO_3{\cdot}20PbO$. The corresponding ΔT_g increases from 24 to 36 °C for each 10 mol TeO_2 substituted by 10 mol WO_3. The glasses of the composition series $(90-x)TeO_2{\cdot}xWO_3{\cdot}10PbO$ (which contain 10 mol WO_3 more and 10 mol PbO less) are different from the glasses of the former series in the sense that, for the same TeO_2 molar percentages, they show higher T_g values (between 28 and 47 °C). Nevertheless, the slope of the corresponding straight line is smaller, since the T_g of glasses only increases 25 °C for each 10 mol TeO_2 substituted by 10 mol WO_3. Therefore, both the substitution mol by mol of TeO_2 and PbO by WO_3 yields an increase of T_g. The two former composition series clearly indicate that WO_3 is the most contributing oxide to increase the glass transition temperature. This confirms that W^{6+}-ions would be incorporated as network formers, either with octahedral coordination [WO_6] or tetrahedral coordination [WO_4], alternating with Te^{4+}-ions and forming mixed linkages Te–O–W and W–O–W. In such groups W–O bonds are stronger, due to their higher field intensity. Following Shaltout et al.[8] the formation of mixed linkages Te–O–W is favoured by the fact that both ions possess similar electronegativity values.

In the glass series with constant molar percentage of WO_3, the substitution of 10 mol PbO mol by mol by 10 mol TeO_2 causes a slight decrease of $\Delta T_g = 6$ °C for 30 mol% WO_3. For 20 mol% WO_3 ΔT_g slightly increases (2–4 °C), and for 10 mol% WO_3 ΔT_g increases even more (11 °C). That is,

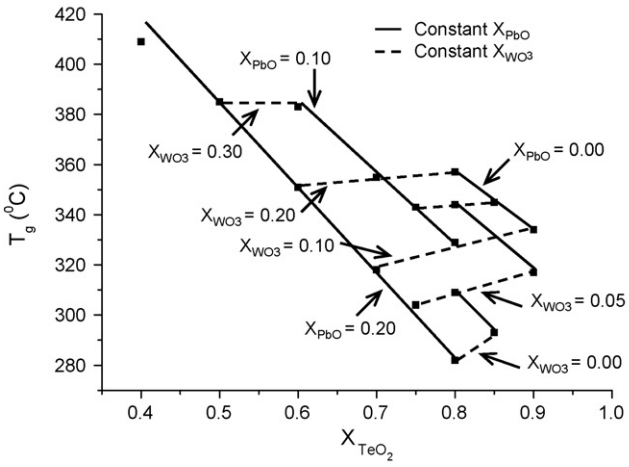

X_{WO3}	Slope
0.05	85.7
0.10	80.0
0.15	20.0
0.20	30.0
X_{PbO}	Slope
0.00	-230
0.10	-269
0.20	-317

Fig. 7. Variation of the transition temperature T_g of glasses as a function of the TeO_2 molar fraction. Continuous fitting lines correspond to constant X_{PbO} and dashed lines to constant X_{WO_3}. Representative values of the obtained slopes are included.

the lower the molar concentration of WO_3, the glass network becomes more relaxed and the contribution of TeO_2 to the increase of T_g becomes more important than that of PbO. This is due to the higher field intensity of Te^{4+}-ions, compared with the field intensity of Pb^{2+}-ions (Table 4). In Fig. 7 the slopes of the linear fits for different values of X_{PbO} and X_{WO_3} are indicated. In the glass series $80TeO_2 \cdot (20-x)WO_3 \cdot xPbO$ with constant 80 mol% TeO_2, the transition temperature always increases when PbO is substituted mol by mol by WO_3.

3.4.2. Thermal stability

The glass forming process needs to avoid any crystallisation during the thermal range in which the forming process takes place. The difference between the onset crystallisation temperature T_c and the glass transition temperature T_g is usually taken as an index to estimate the glass thermal stability. The wider the thermal stability range, the most favoured is the glass forming process.

Calculated thermal stability values for the glasses studied are plotted in Fig. 8a. For a constant TeO_2 percentage, the thermal stability increases when PbO is substituted mol by mol by WO_3. The highest values are reached for glasses containing $[WO_3] \geq 10$ mol%, which corresponds to the marked area in Fig. 8b. This behaviour agrees with the fact that both WO_3 and TeO_2 share the role of network formers in TeO_2–WO_3–PbO glasses for a wide composition range.

3.4.3. Thermal expansion coefficient

In Fig. 9 linear thermal expansion coefficients $\alpha_{100–250°C}$ are plotted as a function of molar fraction X_{TeO_2}. In ternary composition series with constant PbO molar percentage, a strong α decreasing is observed when TeO_2 is substituted mol by mol by WO_3. This behaviour is coherent with the variation of T_g. That is, the glasses showing higher T_g values are those with lower thermal expansion coefficient. This confirms that W^{6+}-ions play as network formers.

For constant TeO_2 molar percentages, α decreases when PbO is substituted by WO_3. On the contrary, α values increase with the molar percentage of modifier Pb^{2+}-ions, as a consequence of

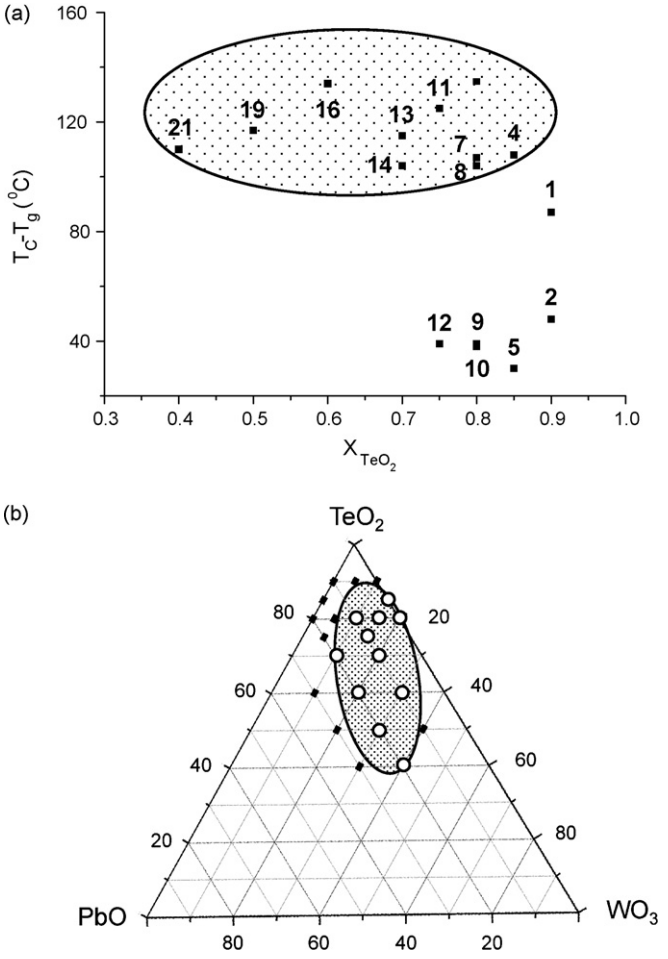

Fig. 8. (a) Thermal stability of the glasses calculated from onset $T_c - T_g$ as a function of X_{TeO_2} and (b) thermal stability of the glasses calculated from onset $T_c - T_g$ in the corresponding ternary diagram.

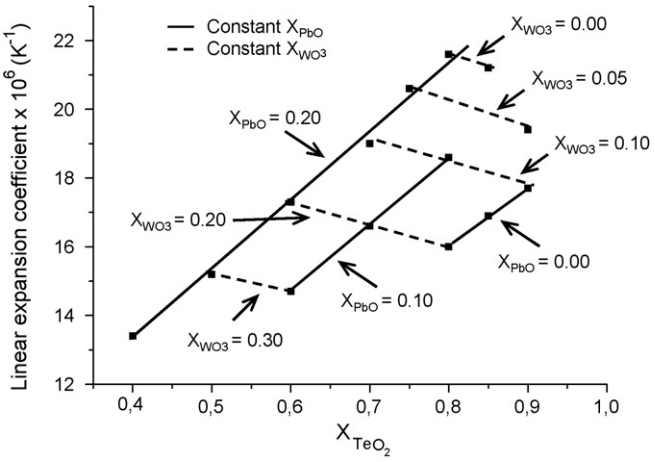

Fig. 9. Variation of the thermal expansion coefficients of glasses as a function of the TeO_2 molar fraction.

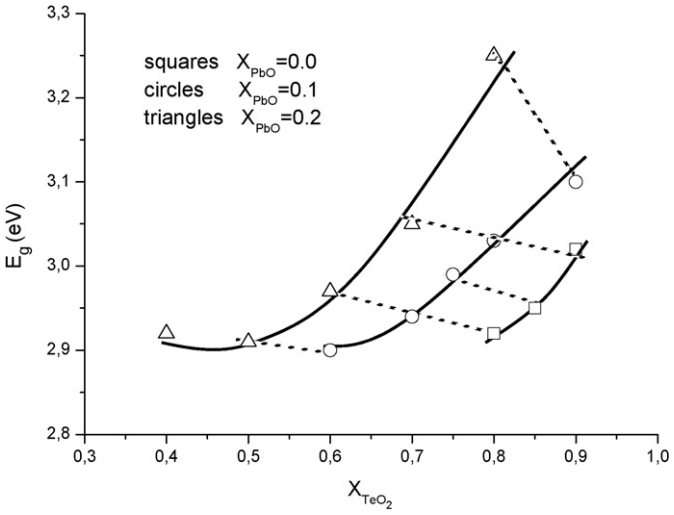

Fig. 10. Variation of the energy gap E_g of glasses as a function of the TeO_2 molar fraction.

the network connectivity decreasing caused by the non-bridging oxygens formation. For the same reason, in the binary system TeO_2–PbO, α values increase when the molar percentage of PbO increases from 15 to 20 mol%. However, in TeO_2–WO_3 binary glass series, the WO_3 molar percentage increasing causes a decreasing of α. This fact indicates that W^{6+}-ions play as network formers in binary compositions as well, since α should increase if they would play as modifying ions.

The data presented in Fig. 9 show that thermal expansion coefficients vary linearly with the molar percentage of each component for each glass series, i.e. α behaves as an additive magnitude. With the aim to evaluate the contribution of each component to α values, the corresponding additive molar factors have been calculated from a hyperabundant equations system: $f_{TeO_2} = (0.200 \pm 0.001) \times 10^{-6}$, $f_{WO_3} = (-0.005 \pm 0.004) \times 10^{-6}$, $f_{PbO} = (0.275 \pm 0.006) \times 10^{-6}$. According to these results, WO_3 contribution to the glasses thermal expansion coefficient is zero or slightly negative. This agrees with the high strength of W–O bond, as well as with the network forming role of WO_3 attributed above, which yields W–O–W and W–O–Te bonds.

3.5. Optical absorption

The glasses energy gap (E_g) values were calculated from the wavelength of the ultraviolet cut-off. In glasses with constant [PbO] (Fig. 10), the energy gap E_g diminishes when the TeO_2/WO_3 ratio decreases. El Sayed Yousef et al.[32] obtained the same result and attributed the decrease of E_g to the non-bridging oxygen increase, caused by the WO_3 incorporation. This explanation works against the authors' point of view, since the present results demonstrate that W^{6+}-ions are incorporated as glass formers, increasing the network connectivity and diminishing the thermal expansion coefficient.

Although it could be expected the contrary, Eg values also diminish slightly when the TeO_2/PbO ratio increases in glasses with constant [WO_3] (Fig. 10), and this behaviour is even more evident for high WO_3 percentages. In other words, it happens when the percentage of modifier ions Pb^{2+} decreases, i.e. when the number of non-bridging oxygens diminish (ions with the higher polarisability). This explains why in both glass series the energy gap does not depend exclusively on the oxygen polarisability, nor on the cations polarisability (Table 5).[33] For instance, WO_3 that has the less polarisable cation, contributes most to the decrease of E_g, while Pb^{2+}-ions that are the more polarisable contribute less to the decrease of E_g.

Table 5
Energy gap E_g of the TeO_2–WO_3–PbO glass system components.

Oxide	Cation polarisability α_i	E_g (eV)
TeO_2	1.595	3.79
WO_3	0.147	2.70
PbO	3.623	2.80

In glasses with constant [TeO_2] the energy gap E_g also decreases from $80TeO_2{\cdot}20PbO$ to $80TeO_2{\cdot}20WO_3$, and from $70TeO_2{\cdot}10WO_3{\cdot}20PbO$ to $70TeO_2{\cdot}20WO_3{\cdot}10PbO$. This behaviour could be explained taking into account that the substitution of TeO_2 by WO_3 incorporates into the glass network one oxygen more than TeO_2. On the same basis, it could be explained that E_g decreases when PbO is substituted by TeO_2 or WO_3, respectively. The higher the number of oxygen atoms, the higher the glass polarisability and, therefore, the lower the E_g values.

4. Conclusions

W^{6+}-ions are incorporated into tellurite glasses as network formers, alternating with Te^{4+}-ions and forming mixed linkages Te–O–W and W–O–W, which increase the glass network connectivity. The basic trigonal bipyramids [TeO_4] (tbp) structure, as well as the progressive formation of [TeO_3] (tp) units, is maintained in all the glasses studied, even for a TeO_2 content as low as 40 mol%. Nevertheless, the broadening of the main FTIR band at 650 cm^{-1} indicates an increasing network

deformation. Such deformation increases as the TeO_2 content diminishes and the WO_3 content increases. This is explained either by the increase of the $[WO_6]$ groups or by the deeper distortion of such octahedral groups.

Pb^{2+}-ions incorporation does not originate new FTIR bands and their presence does not affect the position of the main wide band at 650 cm^{-1}, which is assigned to symmetric axial vibrations of $Te–O_{ax}$ bonds. Moreover, Pb^{2+}-ions strongly shift the shoulder at 770 cm^{-1} towards 730 cm^{-1}, which could be attributed to the higher polarisability of Pb–O–Te linkages.

The molar volume increases with the molar fraction of WO_3 (the component that incorporates the higher number of oxygens) and decreases with the molar fraction of PbO. However, the oxygen molar volume decreases with the molar fraction of WO_3, due to the higher field intensity of W^{6+}-ions (1.47), respect to the corresponding values for Te^{4+}-ions (0.71) and for Pb^{2+}-ions (0.26–0.27), which causes a more compact packing of oxygen ions.

The transition temperature of all glasses studied varies linearly with the molar fraction of each three components: WO_3 is the oxide that contributes most to increase the glass transition temperature. This confirms that W^{6+}-ions are incorporated as network formers, alternating with Te^{4+}-ions, forming mixed Te–O–W and W–O–W linkages. For the same reason, the higher the molar percentage of WO_3, the lower thermal expansion coefficient.

From the point of view of thermal stability, the glasses with wider temperature range to be formed without crystallisation risk are those with high contents of both TeO_2 and WO_3.

Finally, the energy gap E_g decreases when TeO_2 is substituted mol by mol by WO_3; while for constant TeO_2 concentration, E_g increases by substituting WO_3 mol by mol by PbO.

Acknowledgements

Authors wish to thank the financial support of Spanish Ministry of Education and Science (Projects MAT2005-06508-C02-01 and TEC2005-00074/MIC) and the technical support of Dr. C. Gil (National Glass Centre Foundation, Royal Glass Works. La Granja, Spain) and Mr. F. Agua (Centre for Human and Social Sciences, CSIC. Madrid, Spain).

D. Munoz-Martin acknowledges a grant from CSIC-JAE.

References

1. Villegas, M. A. and Fernández Navarro, J. M., Physical and structural properties of glasses in the TeO_2–TiO_2–Nb_2O_5 system. *J. Eur. Ceram. Soc.*, 2007, **27**, 2715–2723.
2. Vogel, W., Bürger, H., Müller, B., Zerge, G., Müller, W. and Forkel, K., Untersuchungen an Telluritgläsern. *Silikattechn*, 1974, **25**, 205–209.
3. Yakhkind, A. K., Tellurite glasses. *J. Am. Ceram. Soc.*, 1966, **49**, 670–675.
4. Al-Ani, S., Hogarth, C. A. and El-Mallawani, R. A., A study of optical-absorption in tellurite and tungsten tellurite glasses. *J. Mater. Sci.*, 1985, **20**, 661–667.
5. Dimitrov, V., Phase-diagram and IR spectral investigations of the $2TeO_2{\cdot}V_2O_5$–$Li_2O{\cdot}V_2O_5{\cdot}2TeO_2$ system. *J. Sol. State Chem.*, 1987, **66**, 256–262.
6. El-Mallawany, R. A., *Tellurite Glasses Handbook*. CRC Press, Boca Raton/London/New York/Washington, DC, 2002.
7. Charton, P., Gengembre, L. and Armand, P., TeO_2–WO_3 glasses: infrared, XPS and XANES structural characterizations. *J. Solid State Chem.*, 2002, **168**, 175–183.
8. Shaltout, I., Tang, Y., Braunstein, R. and Abou-Elazm, A. M., Structural studies of tungstate tellurite glasses by Raman-spectroscopy and differential scanning calorimetry. *J. Phys. Chem. Solids*, 1995, **56**, 141–150.
9. Shaltout, I., Tang, Y., Braunstein, R. and Shaisha, E. E., FTIR spectra and some optical properties of tungstate–tellurite glasses. *J. Phys. Chem. Solids*, 1996, **57**, 1223–1230.
10. Sokolov, V. O., Plotnichenko, V. G. and Dianov, E. M., Structure of WO_3–TeO_2 glasses. *Inorg. Mater.*, 2007, **43**, 194–213.
11. Conti, G. N., Tikhomirov, V. K., Bettinelli, M., Berneschi, S., Brenci, M., Chen, B. *et al.*, Characterization of ion-exchanged waveguides in tungsten tellurite and zinc tellurite Er^{3+}-doped glasses. *Opt. Eng.*, 2003, **42**, 2805–2811.
12. Lim, J. W., Jain, H., Toulouse, J., Marjanovic, S., Sanghera, J. S., Miklos, R. *et al.*, Structure of alkali tungsten tellurite glasses by X-ray photoelectron spectroscopy. *J. Non-Cryst. Solids*, 2004, **349**, 60–65.
13. Luo, Y., Zhang, J., Sun, J., Lu, S. and Wang, X., Spectroscopic properties of tungsten–tellurite glasses doped with Er^{3+} ions at different concentrations. *Opt. Mater.*, 2006, **28**, 255–258.
14. Li, J. C., Li, S. G., Hu, H. F. and Gan, F. X., Emission poperties of Yb^{3+}/Er^{3+} doped TeO_2–WO_3–ZnO glasses for broadband amplifiers. *J. Mater. Sci. Technol.*, 2004, **20**, 139–142.
15. Li, J. C., Xue, T. F., Fan, Y. Y., Li, S. G. and Hu, H. F., Effect of introducing Ce^{3+} on the emission properties of Er^{3+}/Yb^{3+} doped TeO_2–WO_3–ZnO glasses. *Acta Phys. Sin.*, 2006, **55**, 923–928.
16. Shen, X., Nie, Q. H., Xu, T. F. and Gao, Y., Optical transitions of Er^{3+}/Yb^{3+} codoped TeO_2–WO_3–Bi_2O_3 glass. *Spectrochim. Acta Part A: Mol. Biomol. Spectrosc.*, 2005, **61**, 2827–2831.
17. TieFeng Xu, Xiang Shen, QiuHua Nie and Yuan Gao, Spectral properties and thermal stability of Er^{3+}/Yb^{3+} codoped tungsten–tellurite glasses. *Opt. Mater.*, 2006, **28**, 241–245.
18. Zhu, L., Xu, T. F., Nie, Q. H. and Shen, X., Spectral properties and thermal stability of erbium TeO_2–WO_3–La_2O_3 glass. *J. Inorg. Mater.*, 2006, **21**, 351–356.
19. Wang, G., Xu, S., Dai, S., Zhang, J. and Jiang, Z., Thermal stability and spectroscopic properties of Yb^{3+}-doped zinc tungsten tellurite glasses. *J. Alloys Compd.*, 2004, **373**, 246–251.
20. Xiang, S., Nie, X. H., Xu, T. F. and Yuan, G., Investigation of spectral properties and thermal stability of Er^{3+}/Yb^{3+} co-doped tungsten–tellurite glasses. *Acta Phys. Sin.*, 2005, **54**, 2379–2384.
21. Feng, X., Qi, C. H., Lin, F. Y. and Hu, H. F., Tungsten–tellurite glass: a new candidate medium for Yb^{3+}-doping. *J. Non-Cryst. Solids*, 1999, **257**, 372–377.
22. Stanworth, J. E., Tellurite glasses. *J. Soc. Glass Technol.*, 1952, **36**, T217–T241.
23. Heckroodt, R. O. and Res, M. A., Erbium tellurite glasses. *Phys. Chem. Glasses*, 1976, **17**, 217.
24. Afifi, H. and Marzouk, S., Ultrasonic velocity and elastic moduli of heavy metal tellurite glasses. *Mater. Chem. Phys.*, 2003, **80**, 517–523.
25. Afifi, H., Marzouk, S. and Abd el Aal, N., Ultrasonic characterization of heavy metal TeO_2–WO_3–PbO glasses below room temperature. *Physica B*, 2007, **390**, 65–70.
26. Silva, M. A. P., Messadeq, Y., Ribeiro, S. J. L., Poulain, M., Villain, F. and Briois, V., Structural studies of TeO_2–PbO glasses. *J. Phys. Chem. Solids*, 2001, **62**, 1055–1060.
27. Kim, S. H. and Yoko, T., Nonlinear optical properties of TeO_2 based glasses: MO_x–TeO_2 (M = Sc, Ti, V, Nb, Mo, Ta and W) binary glasses. *J. Am. Ceram. Soc.*, 1995, **78**, 1061–1065.
28. Armand, P. and Charton, P., New ternary tellurite glasses: TeO_2–WO_3–Sb_2O_4 and TeO_2–WO_3–Ga_2O_3. *Phys. Chem. Glasses*, 2002, **43**, 291–295.
29. Dimitriev, Y., Dimitrov, V. and Arnaudov, M., IR-spectra and structures of tellurite glasses. *J. Mater. Sci.*, 1983, **18**, 1353–1358.

30. Mizuno, Y., Ikeda, M. and Yoshida, A., Application of tellurite bonding glasses to magnetic heads. *J. Mater. Sci. Lett.*, 1992, **11**, 1653–1656.
31. Tatsumisago, M., Minami, T., Kowada, Y. and Adam, H., Structural-change of rapidly quenched binary tellurite glasses with composition and temperature. *Phys. Chem. Glasses*, 1994, **35**, 89–97.
32. Sayed Yousef, E., El-Adawi, A., El Koshkhany, N. and Shaaban, E. R., Optical and acoustic properties of TeO_2/WO_3 glasses with small amount of additive ZrO_2. *J. Phys. Chem. Solids*, 2006, **67**, 1649–1655.
33. Dimitrov, V. and Sakka, S., Electronic oxide polarizability and optical basicity of simple oxides. *J. Appl. Phys.*, 1996, **79**, 1736–1740.